THE DYNAMICS OF LAPLACE-LIKE RESONANCES

ALESSANDRA CELLETTI, FABRIZIO PAITA, AND GIUSEPPE PUCACCO

Abstract. The Laplace resonance is a three-body dynamical configuration among the Galileian satellites of Jupiter, involving the mean longitudes and the longitudes of perijove of Io, Europa and Ganymede. Beside the classical Laplace resonance, there exists another well known dynamical configuration, to which we refer as the *de Sitter resonance,* which differs from the Laplace resonance in the fact that the longitude of Ganymede is fixed instead of rotating like in the Laplace resonance. The Galileian satellites are characterized by a 2:1 ratio between the mean longitudes of Io-Europa and Europa-Ganymede. We extend the study of the Laplace and de Sitter resonances to the case in which the mean longitudes of the first two satellites are in a ratio $k : j$, while those of the second and third satellites are in a ratio $m : n$ with $k, j, m, n \in \mathbb{Z}_+$ and $|j-k|$, $|n-m| \leq 2$.

We describe the dynamics through a planar Hamiltonian model including the attraction of Jupiter, the mutual interactions of the satellites, the oblateness of Jupiter (limited to the first two even degree zonal harmonic coefficients), and the gravitational influence of the Sun and a fourth satellite (limited to the secular part),which we identify with Callisto when dealing with the Jovian satellites.

In all case studies, we look at the dependence of the resonances on the variation of some observed data, like the semimajor axes of the satellites, the eccentricities, the masses and the oblateness coefficients. The results show that the libration of the Laplace resonant angle is deeply affected by small variations of some quantities, most notably the semimajor axes and the oblateness. Quite surprisingly, in several cases the standard Laplace resonance of the Galileian satellites displays a regular behavior in comparison to other resonances characterized by different mean longitude ratios, which instead show a rather chaotic behavior even on short time scales. This result provides a motivation to support why the Galileian satellites are found in the actual Laplace resonance. We remark that the results on the other Laplace-like resonances can be of interest to explore the dynamics of extra-solar planetary systems.

1. Introduction

The three inner Galileian satellites of Jupiter - Io, Europa, and Ganymede - are observed to move in a particular dynamical configuration, which is commonly known as the *Laplace resonance,* whose precise definition is the following. Let us denote by λ_{Io}, λ_{Eu}, λ_{Ga} the mean longitudes of Io, Europa and Ganymede, and with $\widetilde{\omega}_{Io}$, $\widetilde{\omega}_{Eu}$, $\widetilde{\omega}_{Ga}$

Key words and phrases. Laplace resonance, de Sitter resonance, Chaos, Stability.

The authors acknowledge GNFM/INdAM and the Italian Space Agency for its support through the grant 2013-056-RO.1. A.C. acknowledges the MIUR Excellence Department Project awarded to the Department of Mathematics, University of Rome Tor Vergata, CUP E83C18000100006.

their longitudes of perijoves. The Laplace resonance corresponds to commensurabilities between such quantities, and precisely:

$$\begin{aligned} \lambda_{Io} - 2\lambda_{Eu} + \widetilde{\omega}_{Io} &= 0 \\ \lambda_{Io} - 2\lambda_{Eu} + \widetilde{\omega}_{Eu} &= 180^o \\ \lambda_{Eu} - 2\lambda_{Ga} + \widetilde{\omega}_{Eu} &= 0\ . \end{aligned} \tag{1.1}$$

Let us introduce the *Laplace angle* associated to (1.1) as

$$\Phi_L \equiv \lambda_{Io} - 3\lambda_{Eu} + 2\lambda_{Ga}\ .$$

The condition $\Phi_L = 180^o$ implies that there can never be a triple conjunction of all three satellites. Indeed, the Galileian satellites satisfy the condition $\Phi_L = 180^o$ up to a libration with a small amplitude and period of about 2 071 days ([Lie97], [PCP18]).

The literature on the Laplace resonance is wide and encompasses both analytical theories and numerical integrations. The former aim to build different models for the study of the dynamics (see, e.g. [Lap05], [Sam21], [Mar66], [FM75], [Hen84], [Mal91], [SM97]), while the latter focus on the long-term evolution of the Jovian moons to produce accurate ephemerides (see, e.g., [Lie77], [MVMS02], [LDV04], [Kos09]).

The analytical theories for the dynamics of the Galileian satellites are often aimed to outline specific features, without having to rely necessarily on numerical integrations. Beside the monumental work of Laplace ([Lap05]), we quote [Sam21] which developed an analytical theory to compute quite accurate ephemerides, [dS31] which constructed a theory for the Laplace resonance, [Mar66] which used von Zeipel method to average the short-period terms of the Hamiltonian and to solve the resulting differential equations for the long-period effects, and [FM75] which - revisiting [Lap05] and [Tis96] - obtained the complete first order solution by solving two separate sets of linear integro-differential equations. It is also worth mentioning the works aimed to give an explanation of the origin of the Laplace resonance, very often including tidal effects (see, e.g., [Yod79], [Gre81], [Gre], [Hen83], [YP81], [Mal91]).

In this work, we consider three gravitationally interacting satellites, say S_1, S_2, S_3, moving on the same plane around a planet. The perturbative effects of a fourth satellite and the Sun are also considered. We derive models obtained through a Hamiltonian approach, which include some or all of the following contributions: the Keplerian attraction of Jupiter, the oblateness of the planet, the mutual interactions of the satellites, the gravitational attraction of the fourth satellite and the Sun. The Hamiltonian setting permits to construct models which allow to highlight the role of the different contributions.

Moreover, beside the Laplace resonance, we will consider also variations of (1.1) with different relations between mean longitudes and longitudes of perijoves. We will refer to these relations as *Laplace-like resonances* (see the pioneer work [SM97]); they do not occur in the Solar system, but may found applications in extra-solar planetary systems. In the following sections, we concentrate on resonances which involve combinations of the mean longitudes of the form $j\lambda_{Io} - k\lambda_{Eu}$, $m\lambda_{Eu} - n\lambda_{Ga}$ to which we will refer as $k : j\&m : n$ resonance. In particular, we will consider 5 case studies: $2:1\&2:1$ (namely, the standard Laplace resonance), $3:2\&3:2$, $2:1\&3:2$, $3:1\&3:1$, $2:1\&3:1$.

The Hamiltonian model for the Laplace resonance, including the Keplerian part, the oblateness, the mutual interactions of the satellites, and the gravitational influence of Callisto and the Sun, is presented in Section 2. Such Hamiltonian function is expanded to second order in the eccentricities; beside this function, we introduce also the resonant Hamiltonian.

In addition to resonances of the type (1.1), we also study a different equilibrium solution, which was discovered by de Sitter in [dS31], in which the perijove of Ganymede is librating (see [BZ17], [BH16], [CPP18]), thus showing a different behavior with respect to the standard Laplace resonance (1.1) in which the perijove of Ganymede is rotating.

The de Sitter solution is introduced in Section 3, using a suitable averaged simplified model.

Using such models and definitions of Laplace and de Sitter resonances, in Section 4 we analyze the role of the different terms (precisely, the mutual gravitational influence of the satellites, the oblateness, the attraction of the Sun and a fourth satellite) and the sensitivity of the model to variations of the initial conditions or some parameters (e.g., the semimajor axes of the satellites, the eccentricities, the masses, the oblateness parameter, etc.). To analyze the dynamics we compute a chaos indicator known as Fast Lyapunov Indicator, which provides evidence of the regular and chaotic behavior of the dynamics.

The results show that the actual Laplace resonance is definitely sensitive to variations of the semimajor axis of the inner satellites as well as to the oblateness parameter. This means that an accurate knowledge of the orbital elements and of the physical parameters is mandatory for an exact computation of the libration amplitude of the Laplace angle. This conclusion leads to a careful choice of the model, if one aims to get an accurate prediction of the libration amplitude, also in view of future space missions (e.g., the mission JUICE - JUpiter ICy moons Explorer - planned for lunch in 2022). In addition, we found a characterization of the Laplace resonance in which the Galileian satellites are located, since it results to be much less chaotic with respect to the other resonances ($3:2\&3:2$, $2:1\&3:2$, $3:1\&3:1$, $2:1\&3:1$). This result provides evidence that the actual configuration of the Galileian satellites is indeed the most likely to occur.

2. Hamiltonian model

We consider three point-mass satellites, say S_1, S_2, S_3, orbiting on the same plane around a central planet P and with masses m_1, m_2, m_3. We denote by a_j, e_j, λ_j, $\widetilde{\omega}_j$, respectively, the semimajor axis, eccentricity, mean longitude, and longitude of periapsis of the satellite S_j, $j=1,2,3$. We assume that the semimajor axes are such that $a_1 < a_2 < a_3$ and that the satellites are subject to the following forces:

($H0$) the Keplerian attraction of the planet;
($H1$) the mutual interactions among the satellites S_1, S_2, S_3;
($H2$) the oblateness of the central planet;
($H3$) the gravitational attraction of the Sun;
($H4$) the gravitational influence of a fourth satellite which moves outside the orbit of S_3.

We assume that the osculating orbital elements belong to a collisionless domain, which means that for all values of the orbital elements considered in this paper, collisions will not occur. With such hypotheses, we proceed to write the Hamiltonian function describing the contributions ($H0$)-($H4$). To this end, we need to introduce, as follows, the position vectors in different reference frames:

(i) $\underline{\widetilde{r}}_1$, $\underline{\widetilde{r}}_2$, $\underline{\widetilde{r}}_3$ denote the position vectors of S_1, S_2, S_3 in an inertial reference frame with fixed origin O. We denote by $\underline{\widetilde{r}}_{ij} = \underline{\widetilde{r}}_j - \underline{\widetilde{r}}_i$ the mutual distances;
(ii) $\underline{r}_1$, $\underline{r}_2$, $\underline{r}_3$ denote the position vectors of S_1, S_2, S_3 in a reference frame with axes parallel to the inertial frame, but origin coinciding with the center of mass of the planet.

With this notation, we introduce the so-called Jacobi position vectors $\underline{\rho}_j$, $j=1,2,3$, defined as

$$\underline{\rho}_j = \underline{\widetilde{r}}_j - \frac{1}{\sum_{k=0}^{j-1} m_k} \sum_{k=0}^{j-1} m_k \underline{\widetilde{r}}_k \ ,$$

where m_0 is the mass of the planet and $\underline{\widetilde{r}}_0$ its position vector in the inertial frame. The Jacobi position vectors are the natural coordinates to study the motion of a system like that of the Galileian satellites. However, we will see that at a low order approximation, it will suffice to express the Hamiltonian using planetocentric elements. Introducing the adimensional mass parameter

$$\kappa_j = \frac{m_j}{M_j}\ , \qquad j = 1, 2, 3$$

with $M_1 = m_0 + m_1$, $M_2 = M_1 + m_2$, $M_3 = M_2 + m_3$, we have:

$$\begin{aligned} \underline{\rho}_1 &= \underline{\widetilde{r}}_{01} \\ \underline{\rho}_2 &= \underline{\widetilde{r}}_{02} - \kappa_1 \underline{\rho}_1 \\ \underline{\rho}_3 &= \underline{\widetilde{r}}_{03} - \kappa_1 \underline{\rho}_1 - \kappa_2 \underline{\rho}_2\ . \end{aligned} \tag{2.1}$$

2.1. **Hamiltonian H_{Kep} - Keplerian part.** The Keplerian part describing the interaction between the satellites S_1, S_2, S_3 with the planet, apart a constant term, can be written as

$$H_{Kep} = -\frac{\mathcal{G} M_1 \mu_1}{2a_1} - \frac{\mathcal{G} M_2 \mu_2}{2a_2} - \frac{\mathcal{G} M_3 \mu_3}{2a_3}\ , \tag{2.2}$$

where $\mathcal{G}$ represents the gravitational constant and

$$\mu_1 = \frac{m_0 m_1}{M_1}\ , \qquad \mu_2 = \frac{M_1 m_2}{M_2}\ , \qquad \mu_3 = \frac{M_2 m_3}{M_3}\ .$$

2.2. **Hamiltonian H_{int} - mutual satellites' interactions.** Let us denote by Δ_{jk} the absolute value of the distance vector between S_j and S_k. Then, the Hamiltonian describing the mutual interactions between the satellites can be written as the sum of the *direct* part H'_{int} and the *indirect* part H''_{int}:

$$H_{int} = H'_{int} + H''_{int}\ , \tag{2.3}$$

where (see [Mal91], see also [dS31], [SM97])

$$\begin{aligned} H'_{int} &= -\frac{\mathcal{G} m_1 m_2}{\Delta_{12}} - \frac{\mathcal{G} m_2 m_3}{\Delta_{23}} - \frac{\mathcal{G} m_1 m_3}{\Delta_{13}} \\ &= -\frac{\mathcal{G} m_1 m_2}{|\underline{\rho}_2 - (1-\kappa_1)\underline{\rho}_1|} - \frac{\mathcal{G} m_2 m_3}{|\underline{\rho}_3 - (1-\kappa_2)\underline{\rho}_2|} - \frac{\mathcal{G} m_1 m_3}{|\underline{\rho}_3 - (1-\kappa_1)\underline{\rho}_1 + \kappa_2 \underline{\rho}_2|} \end{aligned} \tag{2.4}$$

and

$$\begin{aligned} H''_{int} &= -\mathcal{G} m_2 (\frac{m_0}{\Delta_{02}} - \frac{M_1}{\rho_2}) - \mathcal{G} m_3 (\frac{m_0}{\Delta_{03}} - \frac{M_2}{\rho_3}) \\ &= -\mathcal{G} M_1 m_2 (\frac{m_0/M_1}{|\underline{\rho}_2 + \kappa_1 \underline{\rho}_1|} - \frac{1}{\rho_2}) - \mathcal{G} M_2 m_3 (\frac{m_0/M_3}{|\underline{\rho}_3 + \kappa_1 \underline{\rho}_1 + \kappa_2 \underline{\rho}_2|} - \frac{1}{\rho_3}) \end{aligned} \tag{2.5}$$

with $\rho_j = |\underline{\rho}_j|$ and $\Delta_{02} = |\underline{\rho}_2 + \kappa_1 \underline{\rho}_1| = |\underline{\widetilde{r}}_2 - \underline{\widetilde{r}}_0|$, $\Delta_{03} = |\underline{\rho}_2 + \kappa_1 \underline{\rho}_1 + \kappa_2 \underline{\rho}_2| = |\underline{\widetilde{r}}_3 - \underline{\widetilde{r}}_0|$. To distinguish between resonant, non-resonant, and secular terms, we need to express the Hamiltonian in terms of the elliptic elements and to perform an expansion of H'_{int} and

H''_{int}, as it is shown in Sections 2.2.1 and 2.2.2 below. The resonant Hamiltonian will then be given in Section 2.2.3.

2.2.1. *Expansion of the direct part H'_{int}.* We start by noticing that from (2.1) it follows that

$$\begin{aligned}
\underline{\rho}_2 - (1-\kappa_1)\underline{\rho}_1 &= \underline{\widetilde{r}}_{02} - \underline{\widetilde{r}}_{01} \\
\underline{\rho}_3 - (1-\kappa_2)\underline{\rho}_2 &= \underline{\widetilde{r}}_{03} - \underline{\widetilde{r}}_{02} \\
\underline{\rho}_3 - (1-\kappa_1)\underline{\rho}_1 + \kappa_2\underline{\rho}_2 &= \underline{\widetilde{r}}_{03} - \underline{\widetilde{r}}_{01} \ ,
\end{aligned}$$

so that (2.4) can be expressed in planetocentric coordinate vectors as

$$H'_{int} = -\frac{\mathcal{G}m_1m_2}{|\underline{\widetilde{r}}_{02} - \underline{\widetilde{r}}_{01}|} - \frac{\mathcal{G}m_2m_3}{|\underline{\widetilde{r}}_{03} - \underline{\widetilde{r}}_{02}|} - \frac{\mathcal{G}m_1m_3}{|\underline{\widetilde{r}}_{03} - \underline{\widetilde{r}}_{01}|} \ . \tag{2.6}$$

Next, we expand in a formal way each of the three terms at the right hand side of (2.6) and then we truncate to a suitable order in the eccentricity. This leads to the following approximation:

$$-\frac{\mathcal{G}m_im_j}{|\underline{\widetilde{r}}_{0j} - \underline{\widetilde{r}}_{0i}|} \ \simeq \ -\frac{\mathcal{G}m_im_j}{a_j}\ \mathcal{R}_D^{(i,j)} \ , \qquad i<j \ ,$$

where $\mathcal{R}_D^{(i,j)}$ denotes the expansion up to the second order in the eccentricity of the term $\frac{a_j}{|\underline{\widetilde{r}}_{0j} - \underline{\widetilde{r}}_{0i}|}$. For self-consistency, following [MD99] we report in Appendix A the explicit expression of the function $\mathcal{R}_D^{(i,j)}$.

2.2.2. *Expansion of the indirect part H''_{int}.* Using (2.5), let us write H''_1 as

$$H''_{int} = H^{(a)}_{int} + H^{(b)}_{int} \ ,$$

where

$$\begin{aligned}
H^{(a)}_{int} &= -\mathcal{G}M_1m_2\ \Big(\frac{m_0/M_1}{|\underline{\widetilde{r}}_{02}|} - \frac{1}{\rho_2}\Big) \ , \\
H^{(b)}_{int} &= -\mathcal{G}M_2m_3\ \Big(\frac{m_0/M_2}{|\underline{\widetilde{r}}_{03}|} - \frac{1}{\rho_3}\Big) \ .
\end{aligned}$$

In practical computations, it is convenient to express the inverse of ρ_2, ρ_3 in planetocentric elements, which can be done by making suitable approximations, as we are going to explain. Indeed, we have:

$$\frac{1}{\rho_2} = \frac{1}{|\underline{\widetilde{r}}_{02}|} + \kappa_1\frac{\underline{\widetilde{r}}_{01}\cdot\underline{\widetilde{r}}_{02}}{|\underline{\widetilde{r}}_{02}|^3} + O(\kappa_1^2) \ ,$$

where

$$\underline{\widetilde{r}}_{01}\cdot\underline{\widetilde{r}}_{02} = |\underline{\widetilde{r}}_{01}|\ |\underline{\widetilde{r}}_{02}|\ \cos\gamma_{12}$$

and where γ_{12} is the angle formed by the radius vectors $\underline{\widetilde{r}}_{01}$ and $\underline{\widetilde{r}}_{02}$. The expansion of $\cos\gamma_{12}$ to second order in the eccentricities is given by the following expression:

$$\begin{aligned}
\cos\gamma_{12} &= (1-e_1^2-e_2^2)\cos(\lambda_1-\lambda_2)+e_1e_2\cos(2\lambda_1-2\lambda_2-\widetilde{\omega}_1+\widetilde{\omega}_2)\\
&+ e_1e_2\cos(\widetilde{\omega}_1-\widetilde{\omega}_2)+e_1\cos(2\lambda_1-\lambda_2-\widetilde{\omega}_1)-e_1\cos(\lambda_2-\widetilde{\omega}_1)\\
&+ e_2\cos(\lambda_1-2\lambda_2+\widetilde{\omega}_2)-e_2\cos(\lambda_1-\widetilde{\omega}_2)+\frac{9}{8}e_1^2\cos(3\lambda_1-\lambda_2-2\widetilde{\omega}_1)\\
&- \frac{e_1^2}{8}\cos(\lambda_1+\lambda_2-2\widetilde{\omega}_1)+\frac{9}{8}e_2^2\cos(\lambda_1-3\lambda_2+2\widetilde{\omega}_2)\\
&- \frac{e_2^2}{8}\cos(\lambda_1+\lambda_2-2\widetilde{\omega}_2)-e_1e_2\cos(2\lambda_1-\widetilde{\omega}_1-\widetilde{\omega}_2)\\
&- e_1e_2\cos(2\lambda_2-\widetilde{\omega}_1-\widetilde{\omega}_2)\ . \qquad (2.7)
\end{aligned}$$

Neglecting terms of order of κ_1^2, we can write

$$H_{int}^{(a)}=-\mathcal{G}\frac{m_1m_2}{|\underline{\widetilde{r}}_{02}|}\ (-1-\frac{|\underline{\widetilde{r}}_{01}|}{|\underline{\widetilde{r}}_{02}|}\cos\gamma_{12})\ .$$

In a similar way, we have:

$$\frac{1}{\rho_3}=\frac{1}{|\underline{\widetilde{r}}_{03}|}+\kappa_1(1-\kappa_2)\frac{\underline{\widetilde{r}}_{01}\cdot\underline{\widetilde{r}}_{03}}{|\underline{\widetilde{r}}_{03}|^3}+\kappa_2\frac{\underline{\widetilde{r}}_{02}\cdot\underline{\widetilde{r}}_{03}}{|\underline{\widetilde{r}}_{03}|^3}+O(\kappa_1^2,\kappa_2^2,\kappa_1\kappa_2)\ .$$

Note that we can write

$$\begin{aligned}
\underline{\widetilde{r}}_{01}\cdot\underline{\widetilde{r}}_{03} &= |\underline{\widetilde{r}}_{01}|\ |\underline{\widetilde{r}}_{03}|\ \cos\gamma_{13}\ ,\\
\underline{\widetilde{r}}_{02}\cdot\underline{\widetilde{r}}_{03} &= |\underline{\widetilde{r}}_{02}|\ |\underline{\widetilde{r}}_{03}|\ \cos\gamma_{23}\ ,
\end{aligned}$$

where the expansions of $\cos\gamma_{13}$, $\cos\gamma_{23}$ are the same as (2.7) with an obvious replacement of the indexes. The expansion of $H_{int}^{(b)}$ to second order in κ_1, κ_2 becomes:

$$H_{int}^{(b)}=-\mathcal{G}\frac{m_1m_3}{|\underline{\widetilde{r}}_{03}|}\ (-1-\frac{|\underline{\widetilde{r}}_{01}|}{|\underline{\widetilde{r}}_{03}|}\cos\gamma_{13})\ -\mathcal{G}\frac{m_2m_3}{|\underline{\widetilde{r}}_{03}|}\ (-1-\frac{|\underline{\widetilde{r}}_{02}|}{|\underline{\widetilde{r}}_{03}|}\cos\gamma_{23})\ .$$

Hence, we obtain

$$\begin{aligned}
H''_{int} &= -\mathcal{G}\frac{m_1m_2}{|\underline{\widetilde{r}}_{02}|}\ (-1-\frac{|\underline{\widetilde{r}}_{01}|}{|\underline{\widetilde{r}}_{02}|}\cos\gamma_{12})-\mathcal{G}\frac{m_1m_3}{|\underline{\widetilde{r}}_{03}|}\ (-1-\frac{|\underline{\widetilde{r}}_{01}|}{|\underline{\widetilde{r}}_{03}|}\cos\gamma_{13})\\
&- \mathcal{G}\frac{m_2m_3}{|\underline{\widetilde{r}}_{03}|}\ (-1-\frac{|\underline{\widetilde{r}}_{02}|}{|\underline{\widetilde{r}}_{03}|}\cos\gamma_{23})\ . \qquad (2.8)
\end{aligned}$$

We consider an expansion of the three terms of H''_{int} in (2.8) to second order in the eccentricities; each term will be approximated as follows:

$$
\begin{aligned}
&- \quad \mathcal{G}\frac{m_i m_j}{\underline{\widetilde{r}}_{0j}}(-1-\frac{|\underline{\widetilde{r}}_{0i}|}{|\underline{\widetilde{r}}_{0j}|}\cos\gamma_{ij}) \simeq \\
&- \quad \mathcal{G}\frac{m_i m_j}{a_j}\ \frac{a_i}{a_j}\ \{(-1+\frac{1}{2}e_i^2+\frac{1}{2}e_j^2)\cos(\lambda_j-\lambda_i)-e_ie_j\cos(2\lambda_j-2\lambda_i-\widetilde{\omega}_j+\widetilde{\omega}_i) \\
&- \quad \frac{e_i}{2}\cos(\lambda_j-2\lambda_i+\widetilde{\omega}_i)+\frac{3}{2}e_i\cos(\lambda_j-\widetilde{\omega}_i)-2e_j\cos(2\lambda_j-\lambda_i-\widetilde{\omega}_j) \\
&- \quad \frac{3}{8}e_j^2\cos(\lambda_j-3\lambda_i+2\widetilde{\omega}_i)-\frac{e_i^2}{8}\cos(\lambda_i+\lambda_j-2\widetilde{\omega}_i)+3e_ie_j\cos(2\lambda_i-\widetilde{\omega}_i-\widetilde{\omega}_j) \\
&- \quad \frac{1}{8}e_j^2\cos(\lambda_i+\lambda_j-2\widetilde{\omega}_j)+\frac{27}{8}e_j^2\cos(3\lambda_j-\lambda_i-2\widetilde{\omega}_j)\}\ .
\end{aligned}
$$

2.2.3. *The resonant Hamiltonian H_{int}^{res}.* As we will see in Section 3, we are interested in resonant motions involving specific linear combinations with integer coefficients of the mean longitudes. More precisely, we will be interested in terms involving the combinations $k\lambda_1 - j\lambda_2$, $m\lambda_2 - n\lambda_3$ with $k, j, m, n \in \mathbb{Z}_+$. In this case, we say that the system satisfies a $j : k$ & $m : n$ resonance. Since we consider the expansion of the perturbing function up to second order in the eccentricities, the resonant Hamiltonian takes the following form:

$$
\begin{aligned}
H_{int}^{res} \quad = \quad & -\sum_{i,j=1}^{3}\frac{\mathcal{G}m_im_j}{a_j}\Big\{A_0^{sec}(\underline{a},\underline{e},\underline{\widetilde{\omega}})+A_1^{res}(\underline{a},\underline{e},\underline{\widetilde{\omega}})\cos(k\lambda_1-j\lambda_2+\widetilde{\omega}_1) \\
& + \quad A_2^{res}(\underline{a},\underline{e},\underline{\widetilde{\omega}})\cos(k\lambda_1-j\lambda_2+\widetilde{\omega}_2)+A_3^{res}(\underline{a},\underline{e},\underline{\widetilde{\omega}})\cos(k\lambda_1-j\lambda_2+2\widetilde{\omega}_1) \\
& + \quad A_4^{res}(\underline{a},\underline{e},\underline{\widetilde{\omega}})\cos(k\lambda_1-j\lambda_2+2\widetilde{\omega}_2)+A_5^{res}(\underline{a},\underline{e},\underline{\widetilde{\omega}})\cos(k\lambda_1-j\lambda_2+\widetilde{\omega}_1+\widetilde{\omega}_2) \\
& + \quad A_6^{res}(\underline{a},\underline{e},\underline{\widetilde{\omega}})\cos(m\lambda_2-n\lambda_3+\widetilde{\omega}_2)+A_7^{res}(\underline{a},\underline{e},\underline{\widetilde{\omega}})\cos(m\lambda_2-n\lambda_3+\widetilde{\omega}_3) \\
& + \quad A_8^{res}(\underline{a},\underline{e},\underline{\widetilde{\omega}})\cos(m\lambda_2-n\lambda_3+2\widetilde{\omega}_2)+A_9^{res}(\underline{a},\underline{e},\underline{\widetilde{\omega}})\cos(m\lambda_1-n\lambda_2+2\widetilde{\omega}_3) \\
& + \quad A_{10}^{res}(\underline{a},\underline{e},\underline{\widetilde{\omega}})\cos(m\lambda_2-n\lambda_3+\widetilde{\omega}_2+\widetilde{\omega}_3)\Big\}\ ,
\end{aligned}
$$

where we denote for short $\underline{a} = (a_1, a_2, a_3)$ and similarly for $\underline{e}$, $\underline{\widetilde{\omega}}$, and where A_0^{sec}, A_1^{res}, ..., A_{10}^{res} are functions of the orbital elements, whose expressions can be obtained from the expansion of the perturbing function given in Appendix A.

2.3. **Hamiltonian H_{obl} - oblateness of the planet.** As we will see in Section 4, the effect of the oblateness of the planet on a Laplace-like resonance might be very important and therefore it must be definitely included in the Hamiltonian. We will limit ourselves to the secular parts, thus depending only on the even degree zonal harmonic coefficients J_{2k}, $k \geq 1$. Typically, one has a smallness relation between the harmonic coefficients, such that $J_2 \gg J_4 \gg J_6 \gg ...$ Therefore we reduce to consider only the effects of J_2 and J_4. Denoting by b the mean radius of the planet, the secular Hamiltonian H_{obl} including the effect of the oblateness is given, e.g. in [Mal91], and has the following expression:

$$
\begin{aligned}
H_{obl} = \; & - \; \frac{\mathcal{G} M_1 \mu_1}{2a_1} \; [J_2(\frac{b}{a_1})^2(1+\frac{3}{2}e_1^2) - \frac{3}{4}J_4(\frac{b}{a_1})^4(1+\frac{5}{2}e_1^2)] \\
& - \; \frac{\mathcal{G} M_2 \mu_2}{2a_2} \; [J_2(\frac{b}{a_2})^2(1+\frac{3}{2}e_2^2) - \frac{3}{4}J_4(\frac{b}{a_2})^4(1+\frac{5}{2}e_2^2)] \\
& - \; \frac{\mathcal{G} M_3 \mu_3}{2a_3} \; [J_2(\frac{b}{a_3})^2(1+\frac{3}{2}e_3^2) - \frac{3}{4}J_4(\frac{b}{a_3})^4(1+\frac{5}{2}e_3^2)] \; . \qquad (2.9)
\end{aligned}
$$

2.4. **Hamiltonian H_{Sun} and H_{sat} - interactions with the Sun and a fourth satellite.** The gravitational interaction with the Sun and with a fourth satellite, orbiting externally to S_3, will be modeled just by retaining the secular part of the Hamiltonians describing such effects. Let us introduce a suffix σ such that $\sigma = Sun$ means that the elements are associated to the Sun and $\sigma = sat$ means that the elements are referred to the fourth satellite. Then, the Hamiltonian reads as

$$
\begin{aligned}
H_\sigma \; = \; & -\frac{\mathcal{G} m_1 m_\sigma}{a_\sigma}\{\frac{1}{2}b_{1/2}^{(0)}(\frac{a_1}{a_\sigma}) - 1 + \frac{1}{8}\frac{a_1}{a_\sigma}b_{3/2}^{(1)}(\frac{a_1}{a_\sigma})(e_1^2+e_\sigma^2)\} \\
& - \; \frac{\mathcal{G} m_2 m_\sigma}{a_\sigma}\{\frac{1}{2}b_{1/2}^{(0)}(\frac{a_2}{a_\sigma}) - 1 + \frac{1}{8}\frac{a_2}{a_\sigma}b_{3/2}^{(1)}(\frac{a_2}{a_\sigma})(e_2^2+e_\sigma^2)\} \\
& - \; \frac{\mathcal{G} m_3 m_\sigma}{a_\sigma}\{\frac{1}{2}b_{1/2}^{(0)}(\frac{a_3}{a_\sigma}) - 1 + \frac{1}{8}\frac{a_3}{a_\sigma}b_{3/2}^{(1)}(\frac{a_3}{a_\sigma})(e_3^2+e_\sigma^2)\} \qquad (2.10)
\end{aligned}
$$

with H_{Sun} referring to the Sun and H_{sat} to the fourth satellite.

2.5. **Complete and resonant Hamiltonians.** In the following sections we will consider two Hamiltonians, both composed by the contributions given in Sections 2.1-2.4. Following [CPP18], we express such Hamiltonians in modified Delaunay variables defined as

$$
L_i = \mu_i\sqrt{GM_i a_i} \; , \qquad \widetilde{P}_i = L_i\left(1-\sqrt{1-e_i^2}\right) \; , \qquad (2.11)
$$

which admit the conjugate angles λ_i and $p_i = -\widetilde{\omega}_i$. Notice that for small eccentricities we can approximate $\widetilde{P}_i$ with $\widetilde{P}_i = \frac{e_i^2 L_i}{2}$. The two Hamiltonians are defined as follows:

(H_{comp}) The first Hamiltonian, say H_{comp}, consists of the sum of the different contributions $H_{Kep} + H_{int} + H_{obl} + H_{Sun} + H_{sat}$ with H_{Kep} as in (2.2), H_{int} as in (2.3) (with H'_{int}, H''_{int} expanded up to second orders in the eccentricity as in Section 2.2.1, 2.2.2), H_{obl} as in (2.9), H_{Sun} and H_{sat} as in (2.10). Hence, we can shortly write H_{comp} as

$$
H_{comp}(L_1, L_2, L_3, \widetilde{P}_1, \widetilde{P}_2, \widetilde{P}_3) = H_{Kep} + H_{int} + H_{obl} + H_{Sun} + H_{sat} \; .
$$

(H_{res}) The second Hamiltonian is obtained by retaining in H_{comp} only the resonant terms as in Section 2.2.3; we refer to such Hamiltonian as H_{res}. The terms in H_{res} vary according to the specific resonance under study.

3. Laplace and de Sitter-like resonances

The actual Laplace resonance among the Galileian satellites involves a commensurability of the mean motions and a locking of the relative precession of the periapsis of Io and Europa. We underline the well-known fact that in the present Laplace resonance the periapsis of Ganymede is not locked. This is an important feature that distinguishes the Laplace resonance from another equilibrium configuration, known as the *de Sitter resonance* ([BZ17], [BH16], [CPP18], [SM97]). The difference between the two resonances is that in the de Sitter resonance the periapsis of Ganymede is locked.

Notwithstanding the fact that the Galileian satellites actually move in the Laplace resonance, it is nevertheless interesting to investigate the dynamics of the de Sitter resonance; even more, it is interesting to generalize both Laplace and de Sitter resonances by considering commensurability relations different from (1.1). This is indeed the content of this Section, in which the definitions of Laplace and de Sitter resonances are extended to the more general case. Indeed, the generalized resonances will be called of type $j:k\&m:n$, when they involve the following combinations of the mean longitudes: $j\lambda_1 - k\lambda_2$, $m\lambda_2 - n\lambda_3$. In the next subsections, we will limit to consider low-order resonances, precisely with indexes j, k, m, n, such that $|j-k|, |m-n| \leq 2$. In particular, we will consider the following three resonances: $j:(j-1)\&n:(n-1)$, $j:(j-2)\&n:(n-2)$, $j:(j-1)\&n:(n-2)$ (see Sections 3.1, 3.2, 3.3).

3.1. Resonance $j:(j-1)\&n:(n-1)$.

The expansion of the perturbing function contains the following angles, which are relevant for the study of the $j:(j-1)\&n:(n-1)$ resonance:

$$\begin{aligned}
\widetilde{q}_1 &= j\lambda_2 + (1-j)\lambda_1 - \widetilde{\omega}_1 \\
\widetilde{q}_2 &= j\lambda_2 + (1-j)\lambda_1 - \widetilde{\omega}_2 \\
\widetilde{q}_3 &= n\lambda_3 + (1-n)\lambda_2 - \widetilde{\omega}_3 \\
\widetilde{q}_4 &= n\lambda_3 + (1-n)\lambda_2 - \widetilde{\omega}_2 \ . \qquad (3.1)
\end{aligned}$$

Since the system is 6–dimensional, two more angles should be introduced, but they do not enter the resonant Hamiltonian, which contains - as said before - only $\widetilde{q}_1$, ..., $\widetilde{q}_4$.

Hence, the additional angles $\widetilde{q}_5$, $\widetilde{q}_6$ are cyclic. We define the *Laplace angle* Φ_L as the quantity $\widetilde{q}_4 - \widetilde{q}_2$, namely

$$\Phi_L \equiv n\lambda_3 + (1-n-j)\lambda_2 - (1-j)\lambda_1 \ ,$$

which provides a link between the mean longitudes of the three satellites.

We notice that for the present resonance the leading terms of the expansion of the perturbing function involving $\widetilde{q}_1$, $\widetilde{q}_2$, $\widetilde{q}_3$, $\widetilde{q}_4$ are of first order in the eccentricity. According to the previous distinction between Laplace and de Sitter resonances, we characterize a de Sitter-like resonance as an equilibrium solution in the variables $\widetilde{q}_1$, $\widetilde{q}_2$, $\widetilde{q}_3$, $\widetilde{q}_4$. On the other hand, a Laplace-like resonance is characterized by the fact that $\widetilde{q}_3$ rotates, instead of being a stationary solution.

Notice that the Galileian satellites Io, Europa, and Ganymede satisfy the resonance $j:(j-1)\&n:(n-1)$ with $j=n=2$ and their initial conditions are such that $\widetilde{q}_1 = \widetilde{q}_4 = 0$, $q_2 = -180^o$. As a consequence, we obtain the following relation between the longitudes of perijoves of Io and Europa:

$$\widetilde{q}_1 - \widetilde{q}_2 = \widetilde{\omega}_2 - \widetilde{\omega}_1 = 180^o \ .$$

3.2. **Resonance $j:(j-2)\&n:(n-2)$.** For such resonance, the relevant angles appearing in the expansion of the perturbing function are the following:

$$\begin{aligned}
\widetilde{q}_1 &= j\lambda_2 + (2-j)\lambda_1 - 2\widetilde{\omega}_1 \\
\widetilde{q}_2 &= j\lambda_2 + (2-j)\lambda_1 - \widetilde{\omega}_1 - \widetilde{\omega}_2 \\
\widetilde{q}_3 &= n\lambda_3 + (2-n)\lambda_2 - \widetilde{\omega}_2 - \widetilde{\omega}_3 \\
\widetilde{q}_4 &= n\lambda_3 + (2-n)\lambda_2 - 2\widetilde{\omega}_2 \\
\widetilde{q}_5 &= j\lambda_2 + (2-j)\lambda_1 - 2\widetilde{\omega}_2 \\
\widetilde{q}_6 &= n\lambda_3 + (2-n)\lambda_2 - 2\widetilde{\omega}_3 \ .
\end{aligned} \tag{3.2}$$

We notice that we have four independent angles, since $\widetilde{q}_5$ and $\widetilde{q}_6$ can be expressed as $\widetilde{q}_5 = 2\widetilde{q}_2 - \widetilde{q}_1$, $\widetilde{q}_6 = 2\widetilde{q}_3 - \widetilde{q}_4$. The Laplace angle is defined as

$$\Phi_L \equiv n\lambda_3 + (2-n-j)\lambda_2 - (2-j)\lambda_1 \ .$$

We notice that in this case the leading terms of the expansion of the perturbing function are of the second order in the eccentricity. A de Sitter-Like resonance corresponds to an equilibrium solution in the variables $\widetilde{q}_1$, $\widetilde{q}_2$, $\widetilde{q}_3$, $\widetilde{q}_4$, while in the Laplace-like solution the angle $\widetilde{q}_3$ circulates.

3.3. **Resonance $j : (j-1)\&n : (n-2)$.** The expansion of the perturbing function contains the following angles, which are relevant for the $j : (j-1)\&n : (n-2)$ resonance:

$$\begin{aligned}
\widetilde{q}_1 &= j\lambda_2 + (1-j)\lambda_1 - \widetilde{\omega}_1 \\
\widetilde{q}_2 &= j\lambda_2 + (1-j)\lambda_1 - \widetilde{\omega}_2 \\
\widetilde{q}_3 &= n\lambda_3 + (2-n)\lambda_2 - \widetilde{\omega}_2 - \widetilde{\omega}_3 \\
\widetilde{q}_4 &= n\lambda_3 + (2-n)\lambda_2 - 2\widetilde{\omega}_2 \\
\widetilde{q}_5 &= n\lambda_3 + (2-n)\lambda_2 - 2\widetilde{\omega}_3 \ .
\end{aligned} \tag{3.3}$$

Since the system is 6-dimensional, an additional angle $\widetilde{q}_6$ should be introduced, which is in fact cyclic for the resonant Hamiltonian. We can easily see that $\widetilde{q}_5 = 2\widetilde{q}_4 - \widetilde{q}_3$, which means that the independent coordinates are $\widetilde{q}_1$, $\widetilde{q}_2$, $\widetilde{q}_3$, $\widetilde{q}_4$. The Laplace angle is defined as

$$\Phi_L \equiv n\lambda_3 + (2-n-2j)\lambda_2 - (2-2j)\lambda_1 \ .$$

The leading terms of the expansion of the perturbing function contain powers of first and second order in the eccentricity. A de Sitter-like resonance corresponds to an equilibrium solution of the coordinates $\widetilde{q}_1$, $\widetilde{q}_2$, $\widetilde{q}_3$, $\widetilde{q}_4$, while in the Laplace-like resonance the angle $\widetilde{q}_3$ rotates.

3.4. **Phase portraits of Laplace and de Sitter resonances.** Following [dS31], the de Sitter resonant configuration is obtained by studying the equilibrium points of a simplified model of the satellite's interactions. The detailed procedure can be found in [CPP18] to which we refer for details. Here, for completeness, we give the general idea, which is based on the following analysis of a simplified model. The original 8 degrees of freedom (hereafter DOF) system is reduced by translational symmetry to a 6 DOF system. By transforming to resonant angular variables as in Sections 3.1, 3.2, 3.3, one recognizes that two variables are cyclic, thus obtaining a 4 DOF system. By means of a Lie transformation, one can construct a resonant normal form to describe the reduced dynamics around the equilibrium. To this end, the 4 DOF Hamiltonian is expanded around the equilibrium up to second order in the momenta and retaining at most up to second-order terms in the eccentricities. Through a nearly-integrable canonical transformation, one computes a resonant normal form, which eventually yields a 1 DOF Hamiltonian. This system admits an elliptic fixed point, to which we refer as the *de Sitter equilibrium*. The 1 DOF phase space is then composed by the de Sitter equilibrium surrounded by librational curves; going farther from the equilibrium,

	$2:1\&2:1$	$3:2\&3:2$	$2:1\&3:2$	$3:1\&3:1$	$2:1\&3:1$
q_1	$2\lambda_2-\lambda_1-\widetilde{\omega}_1$	$3\lambda_2-2\lambda_1-\widetilde{\omega}_1$	$2\lambda_2-\lambda_1-\widetilde{\omega}_1$	$3\lambda_2-\lambda_1-2\widetilde{\omega}_1$	$2\lambda_2-\lambda_1-\widetilde{\omega}_1$
q_2	$2\lambda_2-\lambda_1-\widetilde{\omega}_2$	$3\lambda_2-2\lambda_1-\widetilde{\omega}_2$	$2\lambda_2-\lambda_1-\widetilde{\omega}_2$	$3\lambda_2-\lambda_1-\widetilde{\omega}_1-\widetilde{\omega}_2$	$2\lambda_2-\lambda_1-\widetilde{\omega}_2$
q_3	$2\lambda_3-\lambda_2-\widetilde{\omega}_3$	$3\lambda_3-2\lambda_2-\widetilde{\omega}_3$	$3\lambda_3-2\lambda_2-\widetilde{\omega}_3$	$3\lambda_3-\lambda_2-\widetilde{\omega}_2-\widetilde{\omega}_3$	$3\lambda_3-\lambda_2-\widetilde{\omega}_2-\widetilde{\omega}_3$
q_4	$3\lambda_2-2\lambda_3-\lambda_1$	$5\lambda_2-2\lambda_1-3\lambda_3$	$\lambda_1-4\lambda_2+3\lambda_3$	$4\lambda_2-3\lambda_3-\lambda_1-\widetilde{\omega}_1+\widetilde{\omega}_2$	$3\lambda_2-3\lambda_3-\lambda_1+\widetilde{\omega}_2$
q_5	$\lambda_1-\lambda_3$	$\lambda_1-\lambda_3$	$\lambda_1-\lambda_3$	$\lambda_1-\lambda_3$	$\lambda_1-\lambda_3$
q_6	λ_3	λ_3	λ_3	λ_3	λ_3

TABLE 1. Angular coordinates for the different resonances.

the trajectories become rotational (compare with Figure 1). We notice that the actual Laplace resonance among the Galileian satellites corresponds to a rotational trajectory in which the angle $\widetilde{\omega}_3$ ranges between 0^o and 360^o.

In the following we will analyze the resonances $2:1\&2:1$, $3:2\&3:2$, $2:1\&3:2$, $3:1\&3:1$, $2:1\&3:1$. In such cases, the initial data corresponding to the de Sitter-like equilibrium can be computed as follows. According to [CPP18], we consider the Hamiltonian given by the Keplerian part H_{Kep}, the mutual satellites' interactions H_{int}, limited to first order in the eccentricity, and the Hamiltonian H_{obl} describing the oblateness of the planet. Generalizing the results of [Hen84], [Mal91], we introduce the resonant angle variables $q_1,...,q_6$ as defined in Table 1, which are slightly modified with respect to the variables (3.1), (3.2), (3.3), and we denote by $P_1,...,P_6$ the corresponding momenta.

The transformed Hamiltonian H_{TR} becomes of the following form:

$$H_{TR}=H_{TR}(P_1,...,P_6,q_1,...,q_4)\ ;$$

since q_5, q_6 are cyclic, the corresponding momenta P_5, P_6 are integrals of motion, thus leading to a 4-DOF Hamiltonian system.

A de Sitter-like equilibrium corresponds to a stable stationary solution of Hamilton's equations associated to H_{TR}. Precisely, let us write P_4 as

$$P_4=\overline{P}_4+\delta P_4\ ,$$

where $\overline{P}_4$, $P_5=\overline{P}_5$, $P_6=\overline{P}_6$ can be computed from the initial data. Finally, we solve the system of equations

$$\frac{\partial H_{TR}}{\partial P_j}=0\ ,\qquad \frac{\partial H_{TR}}{\partial q_j}=0\ ,\qquad j=1,...,4\ ,$$

to get $\overline{P}_1$, $\overline{P}_2$, $\overline{P}_3$, δP_4, which correspond to the de Sitter-like equilibrium. We will refer to these values as the *de Sitter initial data;* they will be compared in Section 4 to other kinds of initial data. The phase space portraits in the planes (q_3, P_3) given in Figure 1 show different features with the equilibrium located at $q_3 = 0$ or $q_3 = \pi$. The resonances $2:1\&2:1$, $3:2\&3:2$, $2:1\&3:2$ (which are computed with initial data $q_1 = 0$, $q_2 = q_3 = q_4 = \pi$) show an equilibrium at $q_3 = \pi$; on the contrary, the equilibrium is located at $q_3 = 0$ for the $3:1\&3:1$ resonance (with initial data $q_1 = q_4 = \pi$, $q_2 = q_3 = 0$) and for the $2:1\&3:1$ resonance (with initial data $q_1 = q_3 = 0$, $q_2 = q_4 = \pi$).

4. Sensitivity to variations of elements and parameters

The behavior of the different resonances as some data, like semimajor axes, eccentricities, and masses, are varied, is an important indicator of the probability of finding Galileian-like satellites in a Laplace-like resonance. Such analysis is the content of this Section, where we study in detail the case of the $2:1\&2:1$ resonance, namely the classical resonance that occurs within the Galileian satellites of Jupiter; hence, all values of the parameters and initial data will pertain to the system Io-Europa-Ganymede as the satellites, to Jupiter as the planet with the further attraction of Callisto and the Sun. The other cases will refer to a virtual system formed by Io, Europa, Ganymede, but formally residing in the other resonances. Again a fourth satellite and the Sun are added to get a model close to the observed Galileian satellites' system.

4.1. **Resonance $2:1\&2:1$.** The $2:1\&2:1$ Laplace resonance of the Galileian satellites is characterized by the following relations:

$$\begin{aligned} \lambda_1 - 2\lambda_2 + \widetilde{\omega}_1 &= 0 \\ \lambda_1 - 2\lambda_2 + \widetilde{\omega}_2 &= 180^o \\ \lambda_2 - 2\lambda_3 + \widetilde{\omega}_2 &= 0\ . \end{aligned} \tag{4.1}$$

We will base our computations on a model limited to the resonant Hamiltonian H_{res}; later we will analyze the complete Hamiltonian and compare it with the resonant one (see Section 2.5). To analyze the dependence of the resonance upon the initial conditions and parameters, we let some quantities vary, e.g. a_1, a_2, a_3, m_1, e_1, etc. Let us generically denote by η one of such quantities. We say that *η varies around η_c within a range of size δ*, if the following values are considered:

$$\eta = \eta_c\ (1 - \delta\ \frac{k}{3})\ , \qquad k = -3, ..., 3\ . \tag{4.2}$$

The choice of taking k between -3 and 3 is obviously arbitrary and it is motivated by the need of displaying a reasonable number of curves in the following figures.

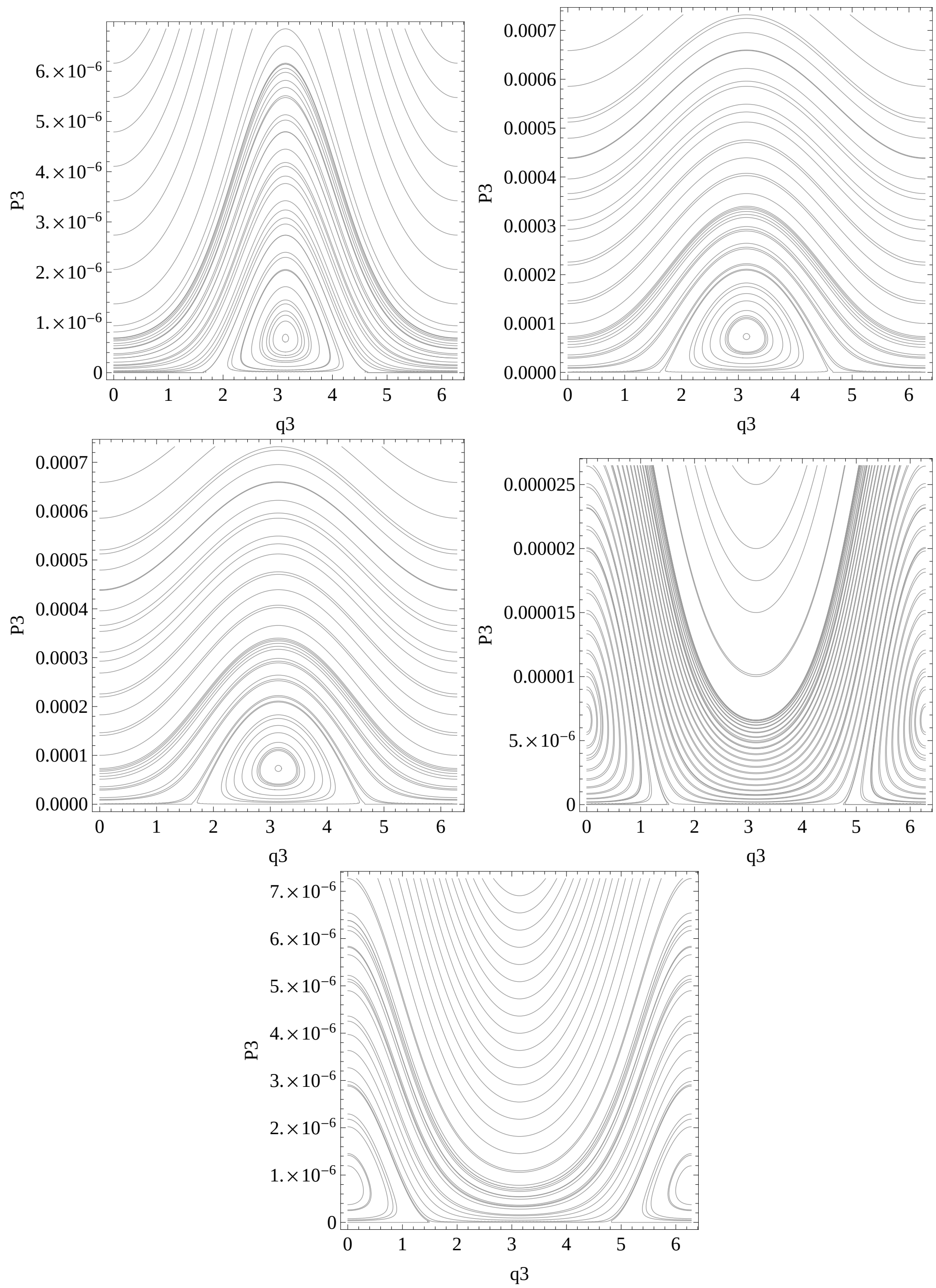

FIGURE 1. Phase space in the (q_3, P_3) plane: upper left resonance $2:1\&2:1$, upper right resonance $3:2\&3:2$, middle left resonance $2:1\&3:2$, middle right resonance $3:1\&3:1$, bottom resonance $2:1\&3:1$.

The panels of Figure 2 shows the variation of the Laplace angle with time, say $\Phi_L = \Phi_L(t)$ defined in Sections 3.1, 3.2, 3.3, over a time span of 10 years; the three panels of Figure 2 show three different choices of the initial conditions as we explain below. In each panel, the semimajor axis of the inner satellite, say S_1 is varied around the observed value of Io, namely (see (4.2))

$$a_1 = a_{Io}(1 - 10^{-4}\ \frac{k}{3})\ , \qquad k = -3, ..., 3\ , \tag{4.3}$$

where a_{Io} is given in Table 2 (we refer to a_{Io}, a_{Eu}, a_{Ga}, respectively, as the effective semimajor axes of Io, Europa, Ganymede as in Table 2; same notation is used for the masses and eccentricities).

In the left panel of Figure 2 we consider the angles corresponding to the position given by the NASA's Spice toolkit[1] at the epoch J2000:

$$\lambda_j^{(0)} = M_j^{(0)} + \omega_j^{(0)} + \Omega_j^{(0)}\ , \qquad \widetilde{\omega}_j^{(0)} = \omega_j^{(0)} + \Omega_j^{(0)}\ , \qquad j = 1, 2, 3\ , \tag{4.4}$$

where the mean anomaly $M_j^{(0)}$, the argument of perijove $\omega_j^{(0)}$, the longitude of the ascending node $\Omega_j^{(0)}$ are given in Table 3. Since we take the observed (and not the theoretical) initial data, the resonance relations (4.1) are satisfied only approximately.

As for the momenta (see (2.11)), we define the initial values through the following relations:

$$\begin{aligned}
L_1^{(0)} &= \frac{m_1}{\sqrt{1+\frac{m_1}{m_0}}}\sqrt{a_1^{(0)}} & \qquad \widetilde{P}_1^{(0)} &= \frac{m_1}{2\sqrt{1+\frac{m_1}{m_0}}}\sqrt{a_1^{(0)}}\,(e_1^{(0)})^2 \\
L_2^{(0)} &= \frac{m_2(1+\frac{m_1}{m_0})}{\sqrt{1+\frac{m_1}{m_0}+\frac{m_2}{m_0}}}\sqrt{a_2^{(0)}} & \qquad \widetilde{P}_2^{(0)} &= \frac{m_2(1+\frac{m_1}{m_0})}{2\sqrt{1+\frac{m_1}{m_0}+\frac{m_2}{m_0}}}\sqrt{a_2^{(0)}}\,(e_2^{(0)})^2 \\
L_3^{(0)} &= \frac{m_3(1+\frac{m_1}{m_0}+\frac{m_2}{m_0})}{\sqrt{1+\frac{m_1}{m_0}+\frac{m_2}{m_0}+\frac{m_3}{m_0}}}\sqrt{a_3^{(0)}} & \qquad \widetilde{P}_3^{(0)} &= \frac{m_3(1+\frac{m_1}{m_0}+\frac{m_2}{m_0})}{2\sqrt{1+\frac{m_1}{m_0}+\frac{m_2}{m_0}+\frac{m_3}{m_0}}}\sqrt{a_3^{(0)}}\,(e_3^{(0)})^2\ .
\end{aligned} \tag{4.5}$$

We will refer to (4.4)-(4.5) as the *SPICE initial data*.

In the middle panel of Figure 2 we consider another set of initial values for the angles, so that the relations (4.1) are exactly satisfied:

$$\begin{aligned}
\lambda_1^{(0)} &= 180^o\ , \qquad \lambda_2^{(0)} = 0\ , \qquad \lambda_3^{(0)} = 0\ , \\
\widetilde{\omega}_1^{(0)} &= 180^o\ , \qquad \widetilde{\omega}_2^{(0)} = 0\ , \qquad \widetilde{\omega}_3^{(0)} = 180^o\ ,
\end{aligned} \tag{4.6}$$

[1] $https://naif.jpl.nasa.gov/naif/toolkit.html$

Satellite	a (km)	e	m (kg)
Io	$4.2203882986903 \cdot 10^5$	$4.7208185639340 \cdot 10^{-3}$	$8.933 \cdot 10^{22}$
Europa	$6.7125250305998 \cdot 10^5$	$9.8185368937703 \cdot 10^{-3}$	$4.797 \cdot 10^{22}$
Ganymede	$1.0705037596264 \cdot 10^6$	$1.4579323465886 \cdot 10^{-3}$	$1.482 \cdot 10^{23}$
Callisto	$1.8827839962701 \cdot 10^6$	$7.4398613187732 \cdot 10^{-3}$	$1.076 \cdot 10^{23}$

Table 2. Semimajor axis, eccentricity and mass of the Galileian satellites.

Satellite	M	$\widetilde{\omega}$	Ω
Io	$3.3518221411689 \cdot 10^2$	$2.4307741374309 \cdot 10^2$	$1.6168077294496 \cdot 10^2$
Europa	$3.4542003028421 \cdot 10^2$	$1.8009776174179 \cdot 10^2$	48.941394451402
Ganymede	$2.7727673067818 \cdot 10^2$	72.912113692461	$2.3160572382619 \cdot 10^2$

Table 3. SPICE initial data of the mean anomaly M, argument of perjove ω, longitude of the ascending node Ω (in degrees) of the first three Galileian satellites.

while the momenta are fixed as in (4.5). We refer to the choice (4.5)-(4.6) as the *Laplace initial data*. As a further choice of the initial values, we proceed as follows: while keeping the data for the angles as in (4.6), we select the initial values of the momenta in the right panel of Figure 2, as the values that correspond to the de Sitter resonance. These data are given by the computations described in Section 3, which yield the initial values of the quantities P_1, ..., P_6. We then multiply P_3 by a factor 10, so to take an initial value which does not correspond exactly to the equilibrium, although still belonging to the libration region around the de Sitter equilibrium. We refer to this choice of the initial conditions as the *de Sitter initial data*.

We specify that, beside the values provided in Tables 2 and 3, we take the masses of the planet and the Sun as $m_P = 1.8986 \cdot 10^{27}\, kg$, $m_{Sun} = 1.9885 \cdot 10^{30}\, kg$, the mean radius of the planet as $b = 71492\, km$, the planet-Sun distance as $a_{PS} = 7.4281042937352 \cdot 10^8\, km$ and the values of the first two zonal harmonic coefficients as $J_2 = 1.478 \cdot 10^{-2}$ and $J_4 = -5.87 \cdot 10^{-4}$. With this choice we have identified the planet with Jupiter, since all data correspond to those of Jupiter.

From the left and middle panels of Figure 2, we infer that a variation of the semimajor axis of S_1 provides drastic changes in the behavior of the Laplace angle with excursions even larger than 20^o, although there is not much difference by taking SPICE and Laplace initial data (compare Figure 2 left and middle). When we are close to the de Sitter equilibrium, then a change in a_1 does not provoke any substantial variation of the Laplace angle (Figure 2, right panel, where all curves overlap to the accuracy of the plot). These

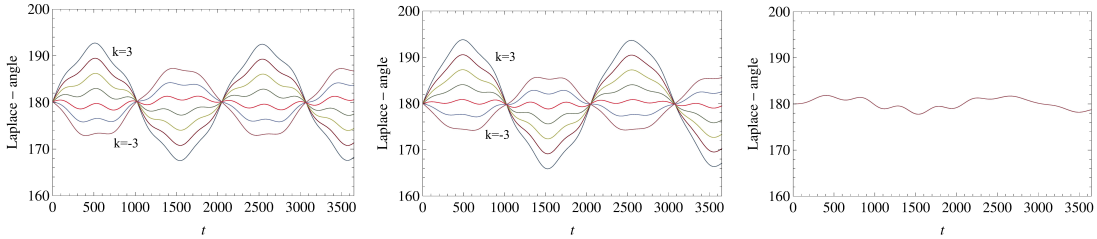

FIGURE 2. Resonance 2 : 1&2 : 1. Time evolution of the Laplace angle Φ_L corresponding to an integration of 10 years with a_1 varied around a_{Io} within a range of size 10^{-4}. Left: SPICE initial data. Middle: Laplace initial data. Right: de Sitter initial data.

results make clear that an accurate knowledge of the initial value of the semimajor axis of the inner satellite is mandatory to obtain a proper evaluation of the libration's amplitude of the Laplace angle of the actual Galileian satellites (compare with [PCP18]).

The effect of varying the semimajor axes of S_2 and S_3 (in our case coinciding with Europa and Ganymede) is similar and it is shown in Figure 3, where the left panel refers to the variation of a_2, while the right panel to that of a_3 (the initial conditions are those of the middle panel of Figure 2, namely Laplace initial data). The effect of the variation of a_2 is more important than that of a_1 and definitely of a_3, a result that we could have expected, since S_2 is in resonance with both S_1 and S_3.

Beside the Laplace angle, we look next at the variation of the other elements. The changes of semimajor axes and eccentricities as the reference value of a_1 varies are given in Figure 4, top panels, which make it evident that the semimajor axes and eccentricities are not heavily affected by changes of a_1, when compared to the effect on the Laplace angle. Very tiny variations of the Laplace angle are provoked by a change of $m_1 = m_{Io}(1-10^{-1}\,\frac{k}{3})$ and $e_1 = e_{Io}(1 - 10^{-2}\,\frac{k}{3})$, $k = -3, ..., 3$, as shown in Figure 4, middle panels. The effect of the variation of J_2 is provided in the bottom panels of Figure 4, where on the left it is $J_2 = J_2^{Jup}(1 - 10^{-2}\,\frac{k}{3})$ and on the right it is $J_2 = J_2^{Jup}(1 - 10^{-1}\,\frac{k}{3})$, where we recall that J_2^{Jup} is the value of J_2 for Jupiter. In the first case the behavior of the Laplace angle is not much affected by the change of J_2 (Figure 4, bottom left panel), while for a larger variation of J_2 there is a marked displacement by taking different values of J_2 (Figure 4, bottom right panel).

The results provided so far are based on the analysis of the resonant Hamiltonian H_{res}. A comparison with the complete Hamiltonian, expanded to second order of the eccentricities, is given in Figure 5. To highlight the similarities and discrepancies between the

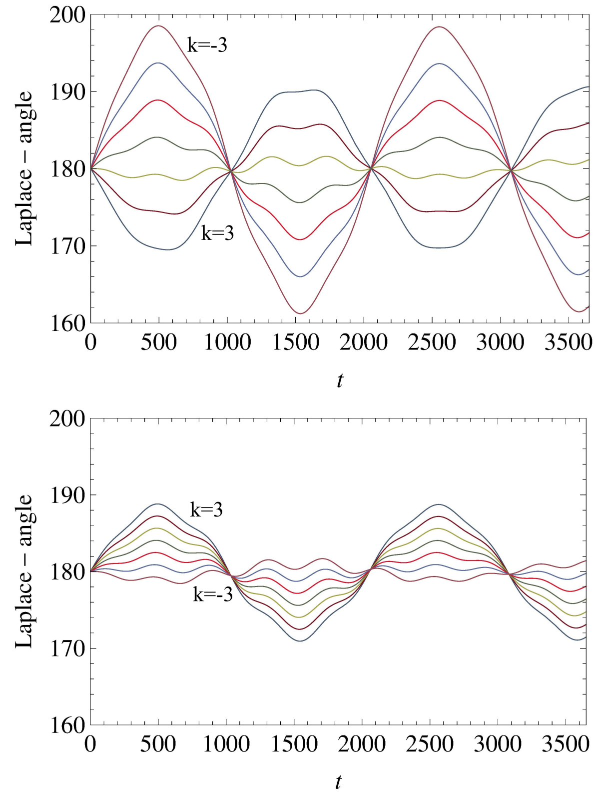

FIGURE 3. Resonance 2 : 1&2 : 1. Time evolution of the Laplace angle corresponding to an integration of 10 years. Left: a_2 is varied around a_{Eu} within a range of size 10^{-4}, Laplace initial data. Right: a_3 is varied around a_{Ga} within a range of size 10^{-4}, Laplace initial data.

complete and resonant Hamiltonians, only the Keplerian part and the mutual satellites' interactions have been considered, since we know that the effect of the oblateness is intrinsically relevant and it might produce discrepancies which might hidden the difference between the behaviors of the complete and resonant Hamiltonians. Figure 5, left panel, gives the comparisons of the Laplace angle, showing that the complete and resonant Hamiltonians determine a similar behavior with the same period although with different amplitudes. The middle panel of Figure 5 gives the semimajor axes of S_1, S_2, S_3, showing that the results associated to the resonant Hamiltonian are a sort of average of those associated to the complete Hamiltonian. The eccentricities of S_1, S_2, S_3 are given in the right panel of Figure 5, showing a good agreement for S_1, S_3, while some discrepancies appear for S_2, whose eccentricity value is larger than that of the other satellites.

A measure of the contribution of the different terms of the Hamiltonian is given in Figure 6. The integration of the complete Hamiltonian, now including all effects (i.e.,

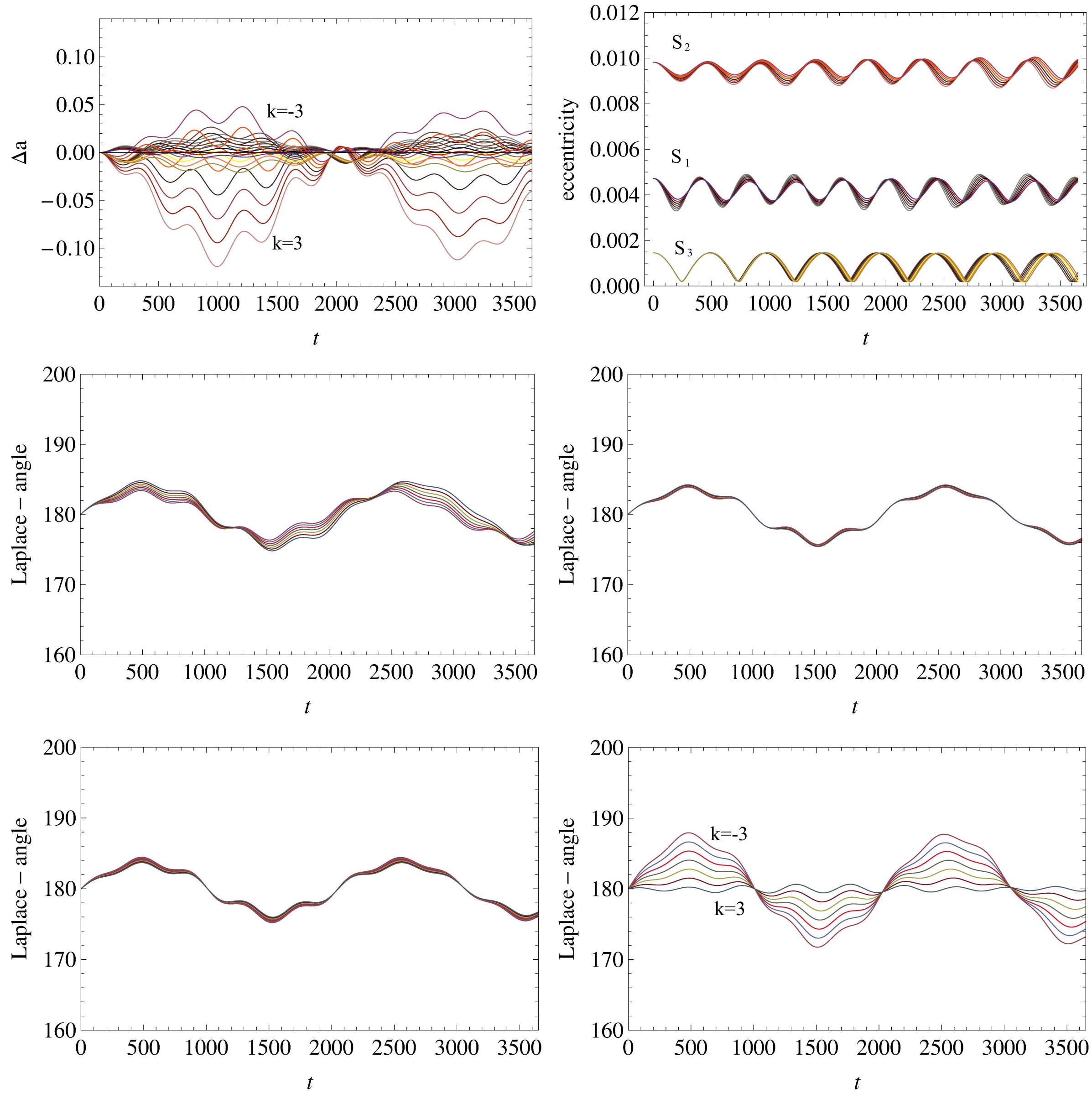

FIGURE 4. Resonance 2 : 1&2 : 1. Top: Time evolution of the difference between the semimajor axis and the reference values given in Table 2 for the 3 satellites (left) and eccentricity of the 3 satellites (right), corresponding to an integration of 10 years and for Laplace initial data with a_1 varied around a_{Io} within a range of 10^{-4}. Middle panels: time evolution of the Laplace's argument corresponding to an integration of 10 years and for Laplace initial data with m_1 varied around m_{Io} within a range of 10^{-1} (left) and e_1 varied around e_{Io} within a range of 10^{-2} (right). Bottom panels: time evolution of the Laplace's argument corresponding to an integration of 10 years and for Laplace initial data with J_2 varied around J_2^{Jup} within a range of 10^{-2} (left) and 10^{-1} (right).

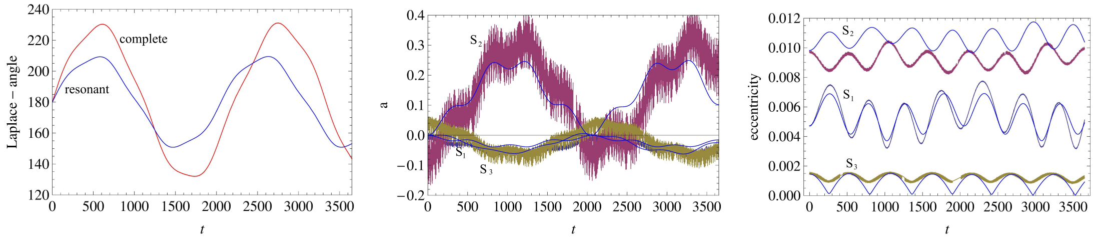

FIGURE 5. Resonance $2:1\&2:1$. Comparison between the resonant and complete Hamiltonians: time evolution of the Laplace's argument (left), semimajor axis (middle) and eccentricity (right) corresponding to an integration of 10 years and for Laplace initial data.

Keplerian part, mutual interactions, oblateness, Sun and Callisto), yields the graph of the Laplace angle in Figure 6, top left panel, while the resonant Hamiltonian gives the result in the top right panel, which is - again - a sort of average behavior of that associated to the complete Hamiltonian. Neglecting the effect of J_4 in the resonant Hamiltonian as in Figure 6, middle left panel, does not provoke significant changes, which are instead very consistent when discarding the effect of J_2 (beside that of J_4) as in Figure 6, middle right panel. This makes clear the role of the oblateness of the planet in shaping the libration of the Laplace angle. Of little significance are the effects of the Sun and the fourth satellite as it can be inferred by comparing the middle right and bottom left panels of Figure 6. Finally, retaining just the secular terms of the mutual satellites' interactions of the Hamiltonian leads to a distortion of the libration curve, as it would have been natural to expect.

4.2. **Other resonances.** To evaluate the likelihood of being in the actual Laplace resonance and to study the dynamics in alternative resonant configurations, we analyze different case studies, corresponding to the $3:2\&3:2$, $2:1\&3:2$ resonances, both containing terms of first order in the eccentricities, the $3:1\&3:1$ case, containing terms of second order in the eccentricities, the $2:1\&3:2$ resonance, containing both first and second order terms in the eccentricities. In all cases the semimajor axes are taken as $a_1 = a_{Io}$, while a_2, a_3 are selected so to satisfy the resonant pair (namely $k:j\&m:n$) and finally we arbitrarily set $a_4 = 3a_3$.

To evaluate the sensitivity of the different resonances to variations of the semimajor axis of the inner satellite, we compute the Fast Lyapunov Indicator ([FLG97]), hereafter FLI, associated to the different semimajor axes corresponding to $a_1 = a_{Io}(1-\delta\ \frac{k}{3})$, $k=-3,...,3$, for typical values of the parameter δ. We recall that the FLI is obtained

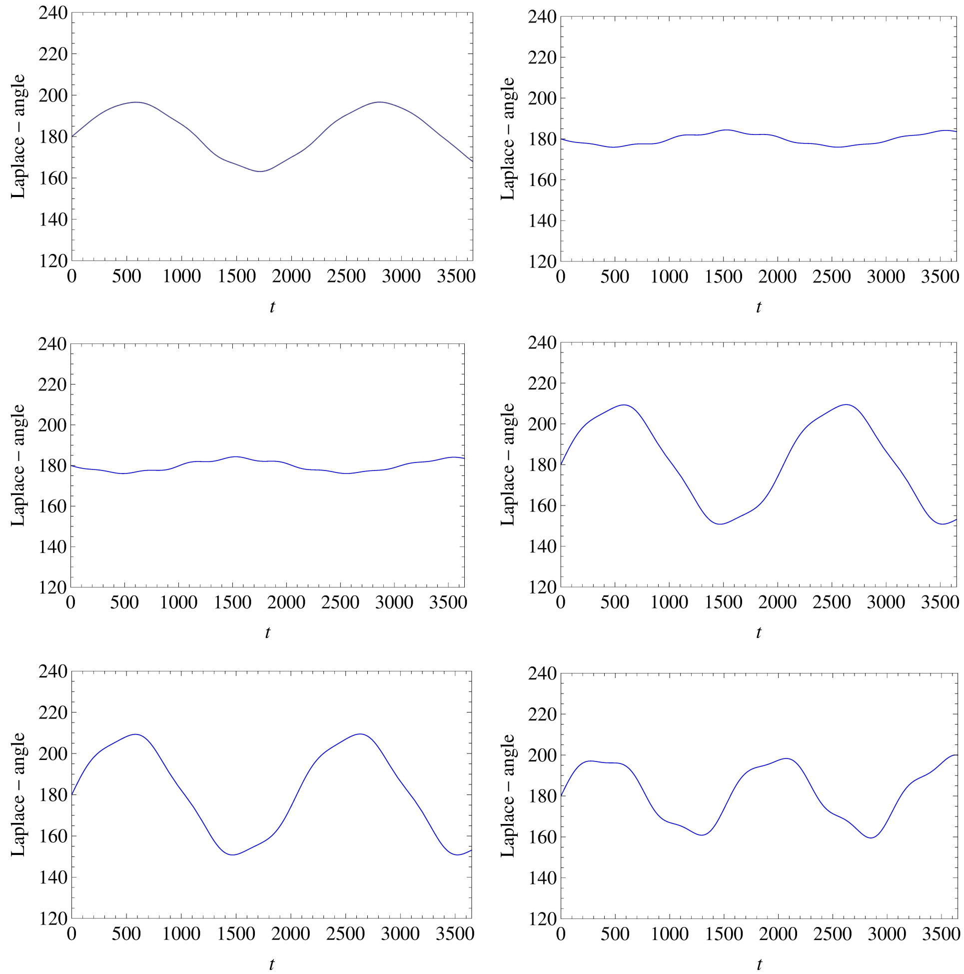

FIGURE 6. Resonance 2 : 1&2 : 1. Time evolution of the Laplace's argument corresponding to an integration of 10 years and for Laplace initial data; all effects are taken into account. Top left: complete Hamiltonian. Top right: resonant Hamiltonian. Middle left: resonant Hamiltonian without J_4. Middle right: resonant Hamiltonian without J_2 and J_4. Bottom left: resonant Hamiltonian without J_2, J_4, Sun and Callisto. Bottom right: resonant Hamiltonian with only secular terms of the mutual satellites' interactions.

by integrating over a finite time the vector field and the variational equations, and by taking the norm of the tangent vector over a finite time interval (see [FLG97]). In all panels of Figures 7 and 8, showing the FLIs, we consider Laplace initial data.

In Figure 7 we give the variation of the Laplace angle on the plots of the left column and the computation of the FLI in the right column. In some cases a regular behavior of the Laplace angle was observed on a given time scale, followed by a chaotic one. To

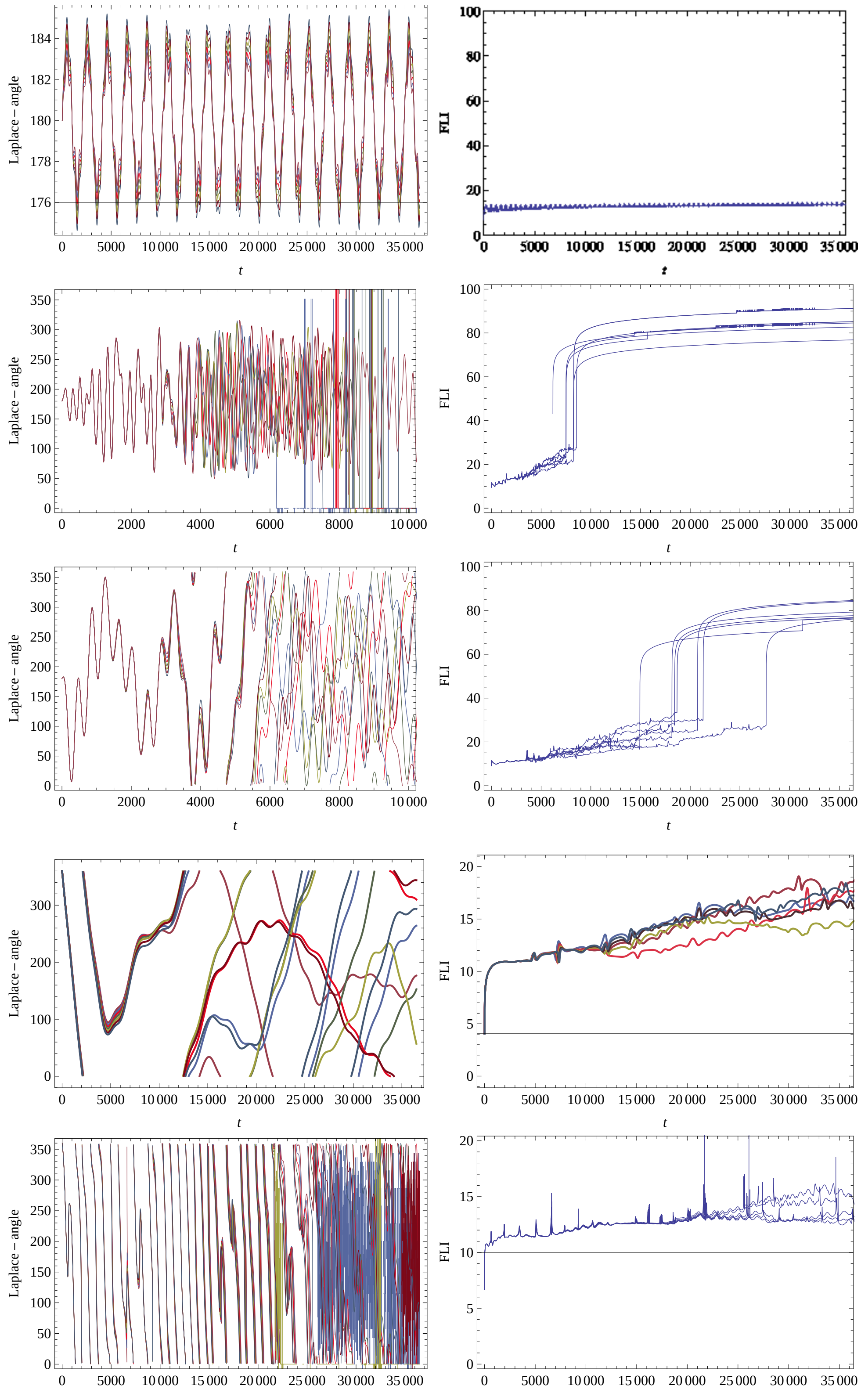

FIGURE 7. Left column: time evolution of the Laplace's argument over 100 years with a_1 varied around a_{Io} within a range of 10^{-5}; right column: computation of the FLI over a time span equal to 36500 days. First row: resonance $2:1\&2:1$, second row: resonance $3:2\&3:2$, third row: resonance $2:1\&3:2$, fourth row: resonance $3:1\&3:1$, fifth row: resonance $2:1\&3:1$.

highlight this phenomenon, in the second and third rows the time scale is limited to 10 000 days, why in all other plots it extends over 36 500 days. The upper panel refers to the 2 : 1&2 : 1 resonance, where a regular behavior is observed, both in terms of the variation of the Laplace angle and the corresponding FLI. A different situation is observed for the 3 : 2&3 : 2 (second row) and 2 : 1&3 : 2 (third row) resonances, where the Laplace angle is librating over a given interval of time (say, 8 000 days for the 3 : 2&3 : 2 resonance and 5 000 days for the 2 : 1&3 : 2 resonance) with a relatively small value of the FLI, followed by a strongly chaotic behavior characterized by large values of the FLI. In the last two cases, 3 : 1&3 : 1 and 2 : 1&3 : 1, the behavior of the Laplace angle and of the FLI denotes a chaotic dynamics, since the beginning of the integration.

Chaos indicators are essential tools to distinguish between regular and chaotic motions. Hence, we explore the behavior of the resonances as the semimajor axis of the inner planet has a wider variation with respect to Figure 7. The results of the computation of the FLI for the different resonances is consistent with the expectation of an increase of chaos, although at different levels, consistently with what we already found in Figure 7. The results are shown in Figure 8, which confirm the higher sensitivity to variations of the inner satellite semimajor axis, with the exception of the 2 : 1&2 : 1 resonance, which displays a very limited chaotic behavior.

5. Laplace vs. de Sitter

As we mentioned in Section 3, the difference between the de Sitter and Laplace configurations resides in the behavior of the angle q_3, which librates in the de Sitter regime, while it circulates in the Laplace regime. Hence, it is definitely interesting to analyze the variation of q_3 with time as some quantities are varied. It turns out that a special role is played by the eccentricities of the satellites. In particular, Figure 9 shows the graph of q_3 over 10 years for a sample of resonances, precisely 2 : 1&2 : 1 (upper row), 2 : 1&3 : 2 (middle row), 3 : 1&3 : 1 (bottom row). In these plots the eccentricities are varied within a range equal to 0.9 (e_1 in the left panels, e_2 in the middle panels, e_3 in the right panels).

A comparison among the different panels of Figure 9 shows that the 2 : 1&2 : 1 resonance is regular to variations of e_1, while it shows a change of behaviors from rotation to libration when varying e_2 and especially e_3. As already noticed in Figures 7 and 8, the other resonances show a very irregular behavior, with transitions from libration to rotation for several values of the eccentricities and even within a single value of the

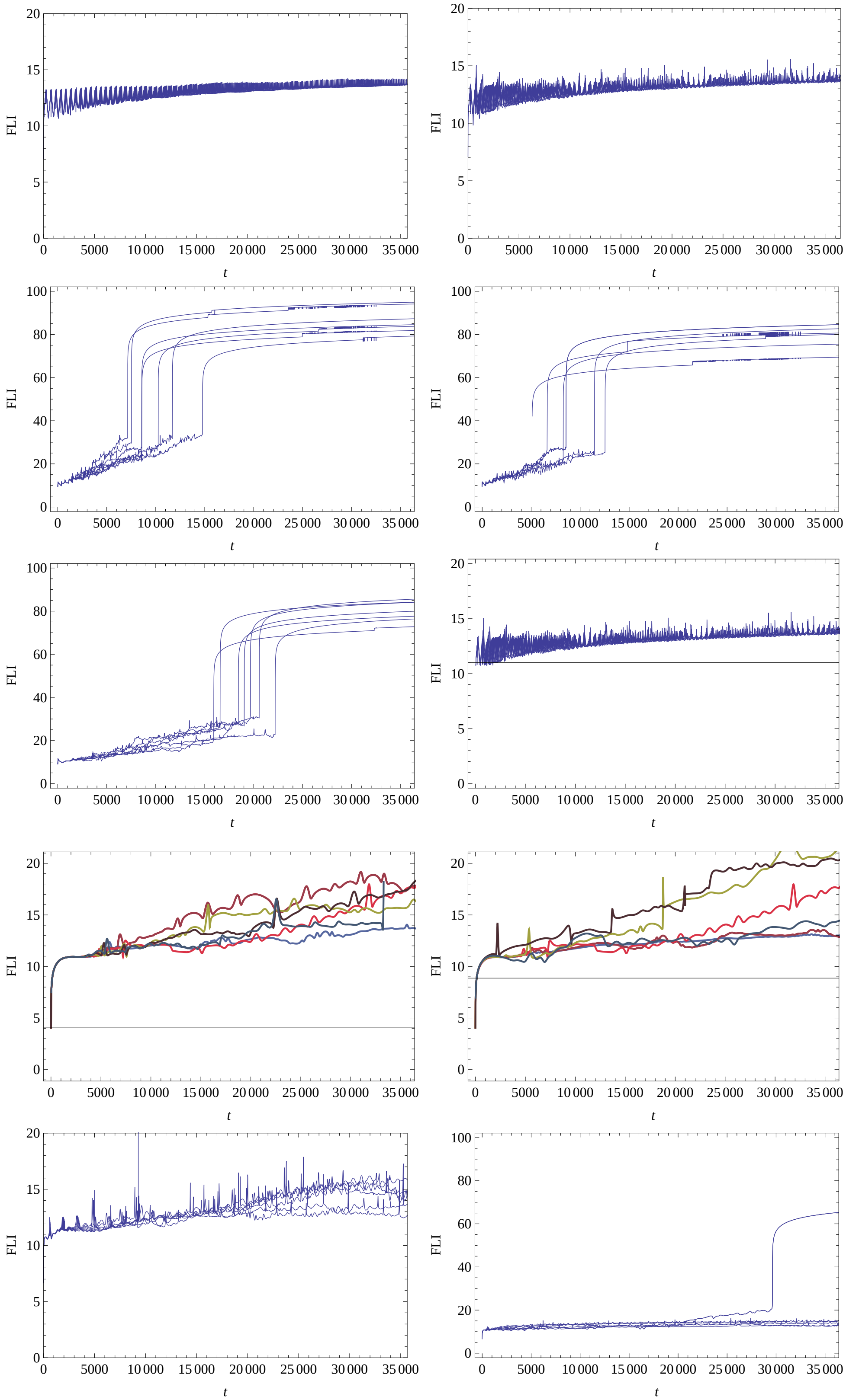

FIGURE 8. FLI over a time span equal to 36500 days with a_1 varied around a_{Io} within a range of 10^{-4} in the left column and 10^{-3} in the right column. First row: resonance $2:1\&2:1$, second row: resonance $3:2\&3:2$, third row: resonance $2:1\&3:2$, fourth row: resonance $3:1\&3:1$, fifth row: resonance $2:1\&3:1$.

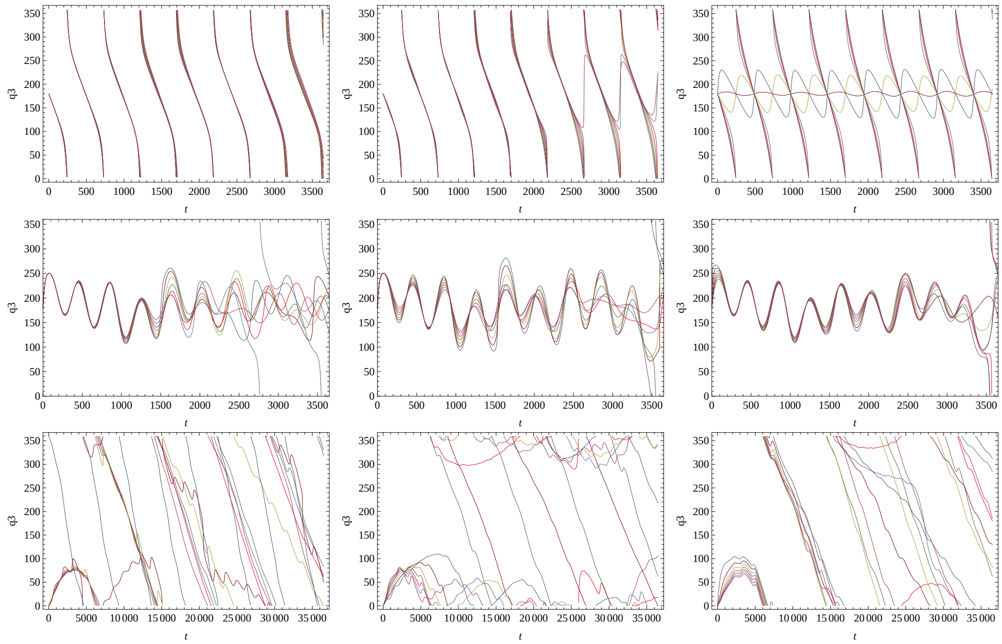

FIGURE 9. Time evolution of the angle q_3 over 10 years for eccentricities varied within a range of 0.9 and Laplace initial data. Top panels: resonance $2:1\&2:1$, middle panels: resonance $2:1\&3:2$, lower panels: resonance $3:1\&3:1$. Left columns: e_1 is varied around e_{Io}, middle columns: e_2 is varied around e_{Eu}, right columns: e_3 is varied around e_{Ga}.

parameters. This is reflected also by the behavior of the angle q_3 for the $2:1\&3:2$ and $3:1\&3:1$ resonances.

Such behavior confirms that the most stable configuration, with respect to variations of the parameters, is the $2:1\&2:1$ resonance, where the Galileian satellites are presently located.

APPENDIX A. EXPANSION OF THE DIRECT PART OF THE PERTURBING FUNCTION

Let $b_s^{(j)}(\alpha)$ denote the Laplace coefficients defined as $b_s^{(j)}(\alpha)=\frac{1}{\pi}\int_0^{2\pi}\frac{\cos(j\psi)d\psi}{(1-2\alpha\cos\psi+\alpha^2)^s}$. Their n-th derivatives $D^n b_s^{(j)}$ can be computed recursively as

$$
\begin{aligned}
Db_s^{(j)} &= s(b_{s+1}^{(j-1)}-2\alpha b_{s+1}^{(j)}+b_{s+1}^{(j+1)})\ ,\\
D^n b_s^{(j)} &= s(D^{n-1}b_{s+1}^{(j-1)}-2\alpha D^{n-1}b_{s+1}^{(j)}+D^{n-1}b_{s+1}^{(j+1)}-2(n-1)D^{n-2}b_{s+1}^{(j)})\ .
\end{aligned}
$$

The expansion of $\mathcal{R}_D^{(i,j)}$ of the direct term $a_j/|\widetilde{\underline{r}}_{0j} - \widetilde{\underline{r}}_{0i}|$ including only terms of second order in the eccentricities (see Section 2.2.1) is given by ([MD99])

$$\mathcal{R}_D^{(i,j)} = -1 + \sum_{k=-4}^{4} \widetilde{R}^{ij}_{D,k} \ ,$$

where $\widetilde{R}^{ij}_{D,k}$ is given by the following expression:

$$\begin{aligned}
\widetilde{R}^{ij}_{D,k} &= (1/2b^k_{\frac{1}{2}}(\alpha_{ij}) - 1/2(e_i^2+e_j^2)k^2b^k_{\frac{1}{2}}(\alpha_{ij}) + 1/4(e_i^2+e_j^2)\alpha_{ij}Db^k_{\frac{1}{2}}(\alpha_{ij}) \\
&+ 1/8(e_i^2+e_j^2)(\alpha_{ij})^2D^2b^k_{\frac{1}{2}}(\alpha_{ij}))\cos(k\lambda_i - k\lambda_j) + (5/16e_i^2kb^k_{\frac{1}{2}}(\alpha_{ij}) + 1/4e_i^2k^2b^k_{\frac{1}{2}}(\alpha_{ij}) \\
&- 1/8e_i^2\alpha_{ij}Db^k_{\frac{1}{2}}(\alpha_{ij}) - 1/4e_i^2k\alpha_{ij}Db^k_{\frac{1}{2}}(\alpha_{ij}) + 1/16e_i^2(\alpha_{ij})^2D^2b^k_{\frac{1}{2}}(\alpha_{ij}))\cos(2\lambda_i + k\lambda_i - 2\widetilde{\omega}_i - k\lambda_j) \\
&+ (1/2e_ikb^k_{\frac{1}{2}}(\alpha_{ij}) - 1/4e_i\alpha_{ij}Db^k_{\frac{1}{2}}(\alpha_{ij}))\cos(\lambda_i + k\lambda_i - \widetilde{\omega}_i - k\lambda_j) \\
&+ (-(5/16)e_i^2kb^k_{\frac{1}{2}}(\alpha_{ij}) + 1/4e_i^2k^2b^k_{\frac{1}{2}}(\alpha_{ij}) - 1/8e_i^2\alpha_{ij}Db^k_{\frac{1}{2}}(\alpha_{ij}) \\
&+ 1/4e_i^2k\alpha_{ij}Db^k_{\frac{1}{2}}(\alpha_{ij}) + 1/16e_i^2(\alpha_{ij})^2D^2b^k_{\frac{1}{2}}(\alpha_{ij}))\cos(2\lambda_i - k\lambda_i - 2\widetilde{\omega}_i + k\lambda_j) \\
&+ (-(1/2)e_ikb^k_{\frac{1}{2}}(\alpha_{ij}) - 1/4e_i\alpha_{ij}Db^k_{\frac{1}{2}}(\alpha_{ij}))\cos(\lambda_i - k\lambda_i - \widetilde{\omega}_i + k\lambda_j) \\
&+ (1/4b^k_{\frac{1}{2}}(\alpha_{ij})e_j - 1/2kb^k_{\frac{1}{2}}(\alpha_{ij})e_j + 1/4\alpha_{ij}Db^k_{\frac{1}{2}}(\alpha_{ij})e_j)\cos(k\lambda_i + \lambda_j - k\lambda_j - \widetilde{\omega}_j) \\
&+ (1/4e_ikb^k_{\frac{1}{2}}(\alpha_{ij})e_j - 1/2e_ik^2b^k_{\frac{1}{2}}(\alpha_{ij})e_j - 1/4e_i\alpha_{ij}Db^k_{\frac{1}{2}}(\alpha_{ij})e_j \\
&+ 1/2e_ik\alpha_{ij}Db^k_{\frac{1}{2}}(\alpha_{ij})e_j - 1/8e_i(\alpha_{ij})^2D^2b^k_{\frac{1}{2}}(\alpha_{ij})e_j)\cos(\lambda_i + k\lambda_i - \widetilde{\omega}_i + \lambda_j - k\lambda_j - \widetilde{\omega}_j) \\
&+ (-(1/4)e_ikb^k_{\frac{1}{2}}(\alpha_{ij})e_j - 1/2e_ik^2b^k_{\frac{1}{2}}(\alpha_{ij})e_j - 1/4e_i\alpha_{ij}Db^k_{\frac{1}{2}}(\alpha_{ij})e_j \\
&- 1/2e_ik\alpha_{ij}Db^k_{\frac{1}{2}}(\alpha_{ij})e_j - 1/8e_i(\alpha_{ij})^2D^2b^k_{\frac{1}{2}}(\alpha_{ij})e_j)\cos(\lambda_i - k\lambda_i - \widetilde{\omega}_i + \lambda_j + k\lambda_j - \widetilde{\omega}_j) \\
&+ (1/4b^k_{\frac{1}{2}}(\alpha_{ij})e_j + 1/2kb^k_{\frac{1}{2}}(\alpha_{ij})e_j + 1/4\alpha_{ij}Db^k_{\frac{1}{2}}(\alpha_{ij})e_j)\cos(k\lambda_i - \lambda_j - k\lambda_j + \widetilde{\omega}_j) \\
&+ (1/4e_ikb^k_{\frac{1}{2}}(\alpha_{ij})e_j + 1/2e_ik^2b^k_{\frac{1}{2}}(\alpha_{ij})e_j - 1/4e_i\alpha_{ij}Db^k_{\frac{1}{2}}(\alpha_{ij})e_j \\
&- 1/8e_i(\alpha_{ij})^2D^2b^k_{\frac{1}{2}}(\alpha_{ij})e_j)\cos(\lambda_i + k\lambda_i - \widetilde{\omega}_i - \lambda_j - k\lambda_j + \widetilde{\omega}_j) \\
&+ (-(1/4)e_ikb^k_{\frac{1}{2}}(\alpha_{ij})e_j + 1/2e_ik^2b^k_{\frac{1}{2}}(\alpha_{ij})e_j - 1/4e_i\alpha_{ij}Db^k_{\frac{1}{2}}(\alpha_{ij})e_j) \\
&\ \cos(\lambda_i - k\lambda_i - \widetilde{\omega}_i - \lambda_j + k\lambda_j + \widetilde{\omega}_j) \\
&+ (-(1/8)e_i(\alpha_{ij})^2D^2b^k_{\frac{1}{2}}(\alpha_{ij})e_j)\cos(\lambda_i - k\lambda_i - \widetilde{\omega}_i - \lambda_j + k\lambda_j + \widetilde{\omega}_j) \\
&+ (1/4b^k_{\frac{1}{2}}(\alpha_{ij})e_j^2 - 9/16kb^k_{\frac{1}{2}}(\alpha_{ij})e_j^2 + 1/4k^2b^k_{\frac{1}{2}}(\alpha_{ij})e_j^2 + 3/8\alpha_{ij}Db^k_{\frac{1}{2}}(\alpha_{ij})e_j^2 \\
&- 1/4k\alpha_{ij}Db^k_{\frac{1}{2}}(\alpha_{ij})e_j^2 + 1/16(\alpha_{ij})^2D^2b^k_{\frac{1}{2}}(\alpha_{ij})e_j^2)\cos(k\lambda_i + 2\lambda_j - k\lambda_j - 2\widetilde{\omega}_j) \\
&+ (1/4b^k_{\frac{1}{2}}(\alpha_{ij})e_j^2 + 9/16kb^k_{\frac{1}{2}}(\alpha_{ij})e_j^2 + 1/4k^2b^k_{\frac{1}{2}}(\alpha_{ij})e_j^2 + 3/8\alpha_{ij}Db^k_{\frac{1}{2}}(\alpha_{ij})e_j^2 \\
&+ 1/4k\alpha_{ij}Db^k_{\frac{1}{2}}(\alpha_{ij})e_j^2 + 1/16(\alpha_{ij})^2D^2b^k_{\frac{1}{2}}(\alpha_{ij})e_j^2)\cos(k\lambda_i - 2\lambda_j - k\lambda_j + 2\widetilde{\omega}_j) \ .
\end{aligned}$$

References

[BH16] H. W. Broer and H. Hanßmann. On Jupiter and his Galilean satellites: Librations of de Sitter's periodic motions. *Indagationes Mathematicae*, 27:1305–1336, 2016.

[BZ17] H. W. Broer and L. Zhao. De Sitter's theory of Galilean satellites. *Cel. Mech. Dyn. Astr.*, 127:95–119, 2017.

[CPP18] A. Celletti, F. Paita, and G. Pucacco. The dynamics of the de Sitter resonance. *Celest. Mech. Dyn. Astr.*, 130(15), 2018.

[dS31] W. de Sitter. Jupiter's Galilean satellites. *Monthly Notices of the Royal Astronomical Society*, 91:706–738, 1931.

[FLG97] C. Froeschlé, E. Lega, and R. Gonczi. Fast Lyapunov Indicators. Application to Asteroidal Motion. *Celestial Mechanics and Dynamical Astronomy*, 67:41–62, January 1997.

[FM75] S. Ferraz-Mello. Problems on the Galilean satellites of Jupiter. *Celestial Mechanics*, 12:27–37, 1975.

[Gre] R. Greenberg. *Satellites of Jupiter*, chapter Orbital Evolution of the Galilean Satellites, pages 65–92. University of Arizona Press.

[Gre81] R. Greenberg. Tidal Evolution of the Galilean Satellites: A Linearized Theory. *Icarus*, 46:415–423, 1981.

[Hen83] J. Henrard. Orbital Evolution of the Galilean Satellites: Capture into Resonance. *Icarus*, 53:55–67, 1983.

[Hen84] J. Henrard. Libration of Laplace's argument in the Galilean satellites theory. *Celestial Mechanics*, 34:255–262, 1984.

[Kos09] G. Kosmodamianskii. Numerical Theory of the Motion of Jupiter's Galilean Satellites. *Solar System Research*, 43(6):465–474, 2009.

[Lap05] P.-S. Laplace. *Traite de mecanique celeste, 4*. Paris : Crapelet ; Courcier ; Bachelier, 1805.

[LDV04] V. Lainey, L. Duriez, and A. Vienne. New accurate ephemerides for the Galilean satellites of Jupiter (I). *Astronomy and Astrophysics*, 420:1171–1183, 2004.

[Lie77] J.H. Lieske. Theory of Motion of Jupiter's Galilean Satellites. *Astronomy and Astrophysics*, 56:333–352, 1977.

[Lie97] J.H. Lieske. Galilean satellites ephemerides E5. *Astronomy and Astrophysics Supplement Series*, 129:205–217, 1997.

[Mal91] R. Malhotra. Tidal Origin of the Laplace Resonance and the Resurfacing of Ganymede. *Icarus*, 94:399–412, 1991.

[Mar66] B.G. Marsden. *The motions of the Galileian satellites of Jupiter*, chapter X, pages 65–92. Yale University PhD thesis, University Microfilms, Inc., Ann Arbor, Michigan, 1966.

[MD99] C. D. Murray and S. F. Dermott. *Solar system dynamics*. Cambridge University Press, 1999.

[MVMS02] S. Musotto, F. Varadi, W. Moore, and G. Schubert. Numerical Simulations of the Orbits of the Galilean Satellites. *Icarus*, 159:500–504, 2002.

[PCP18] F. Paita, A. Celletti, and G. Pucacco. Element history of the Laplace resonance: a dynamical approach. *Astronomy & Astrophysics*, 2018.

[Sam21] R.A. Sampson. Theory of the Four Great Satellites of Jupiter. *Memoirs of the Royal Astronomical Society*, 63:1–270, 1921.

[SM97] A.P. Showman and R. Malhotra. Tidal Evolution into the Laplace Resonance and the Resurfacing of Ganymede. *Icarus*, 127:93–111, 1997.

[Tis96] F. Tisserand. *Traité de Mécanique Céleste*, volume 1, chapter X. Gauthier Ed., 1896.

[Yod79] C.F. Yoder. How tidal heating in Io drives the galilean orbital resonance locks. *Nature*, 279:767–770, 1979.

[YP81] C.F. Yoder and S.J. Peale. The Tides of Io. *Icarus*, 47:1–35, 1981.

Department of Mathematics, University of Roma Tor Vergata, Via della Ricerca Scientifica 1, 00133 Roma (Italy)
E-mail address: celletti@mat.uniroma2.it

Department of Mathematics, University of Roma Tor Vergata, Via della Ricerca Scientifica 1, 00133 Roma (Italy)
E-mail address: f.paita@live.it

Department of Physics, University of Roma Tor Vergata, Via della Ricerca Scientifica 1, 00133 Roma (Italy)
E-mail address: pucacco@roma2.infn.it